

## Electronic Supplementary Information for

### Broadband Photoresponse Based on A Synergetic Effect of Surface Ions and Plasmon Polaritons

*Yu Liu,<sup>a</sup> Jun Yin,<sup>a</sup> Peng-Fei Wang,<sup>a</sup> Jia-Lin Zhu,<sup>a</sup> Wanyun Ma,<sup>a,b,\*</sup> Zhanmin Dong,<sup>c,\*</sup> and Jia-Lin Sun,<sup>a,b,\*</sup>*

- a. State Key Laboratory of Low-Dimensional Quantum Physics, Department of Physics, Tsinghua University, Beijing 100084, P. R. China  
\*Email: mawy@tsinghua.edu.cn (Wanyun Ma);*
- b. Collaborative Innovation Center of Quantum Matter, Beijing, P. R. China  
Email: jlsun@tsinghua.edu.cn (Jia-Lin Sun);*
- c. Department of Physics, Tsinghua University, Beijing 100084, P. R. China  
Email: dongzm@tsinghua.edu.cn (Zhanmin Dong);*

### Calculation of light power density

For the lasers of 405 nm, 532 nm, 633 nm and 1064 nm, their spots meet Gauss distribution. To calculate the equivalent average light power density, we should get the light power irradiated on the effective area. For a light spot meeting Gauss distribution, the total light power within a circular plane rotational symmetric around the optical axis can be expressed as:

$$\frac{P(r)}{P_0} = 1 - e^{(-2r^2/\omega^2)}$$

Where  $r$  is the radius of circle,  $P_0$  is the total light power of spot and  $\omega$  is denoted as the waist radius of laser light beam. The effective area of our device is  $1 \text{ mm} \times 1 \text{ mm}$ , so when we calculated the light power in such a square region we used a circle with radius of 0.56 mm to replace the square approximately. Hence, the light power within the circle is:

$$P(r = 0.56) = P_0 \cdot e^{(-2r^2/\omega^2)}$$

Then we can get the equivalent average light power density (i.e. light intensity) as  $P(r)/A$ , where  $A$  is the area of effective illuminated region ( $1 \text{ mm}^2$ ).

The remained 375 nm laser has a square light spot with dimensions of  $2 \text{ mm} \times 2 \text{ mm}$ . When we calculated the light power density, we assumed the distribution of light intensity is uniform. Then we could get the average light intensity through dividing the total light power by the total area of light spot.

## Au film Absorption

We fabricated a new Au film and measured the absorbance of Au film from 300 nm to 900 nm. The results of absorbance matched well with the results of Ref. 4 and Ref. 5. According to the study of Ref. 3~5, the absorption band in Fig. S1 is attributed to the plasma resonance. Hence, the responsivities of Au film at wavelengths of 375 nm, 405 nm, 532 nm, 633 nm, 785 nm, 808 nm, and 1064 nm matched well with the plasma absorption band.

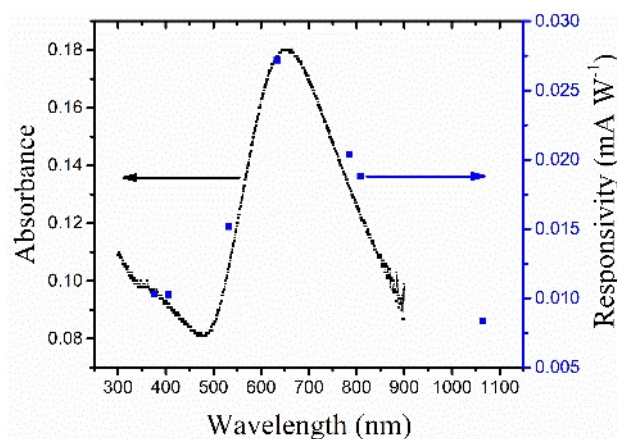


**Fig. S1.** The solid line is an absorption curve of Au film. The square dots are responsivities of Au film.

## The Model of Photoresponse Processes

### Section one. Au<sup>+</sup> ionic diffusion model

First, we divide the region of interest into three parts as Fig. S2 shows. Part I is the illuminated region of Au film, where the Au<sup>+</sup> ionic concentration is denoted as  $C_1$ . Part II is the illuminated region of RbAg<sub>4</sub>I<sub>5</sub>, where the Au<sup>+</sup> ionic concentration is denoted as  $C_2$ . Part III is the region of RbAg<sub>4</sub>I<sub>5</sub> without illumination, where the Au<sup>+</sup> ionic concentration is denoted as  $C_3$ .

The influence of the diffused Au<sup>+</sup> ions is dual as the collected Au<sup>+</sup> ions in RbAg<sub>4</sub>I<sub>5</sub> can scatter the conducting electrons and the lost lattices in Au film can increase the resistance. However, considering the thickness of the Au film, the scattered electrons are the dominant contribution to the negative photoconductivity. Then we display some assumptions to simplify our analysis. 1. When the light power is not strong enough to collect abundant Au<sup>+</sup> ions in RbAg<sub>4</sub>I<sub>5</sub>, we can assume that the changed conductivity of Au film from the scattered electrons is proportional to  $C_2^{1-3}$ . 2. Since the number of the diffused Au<sup>+</sup> ions from Au film to RbAg<sub>4</sub>I<sub>5</sub> is negligible compared with that of the total Au<sup>+</sup> ions in the Au film, we assume the change of  $C_1$  is negligible. 3. Since the total number of Au<sup>+</sup> ions diffused from Part II into Part III is very small, we assume  $C_3$  keeps zero. 4. Since  $C_1$  is much larger than  $C_2$  and  $C_1$  is almost unchanged, we assume  $C_1-C_2$  is time independent.

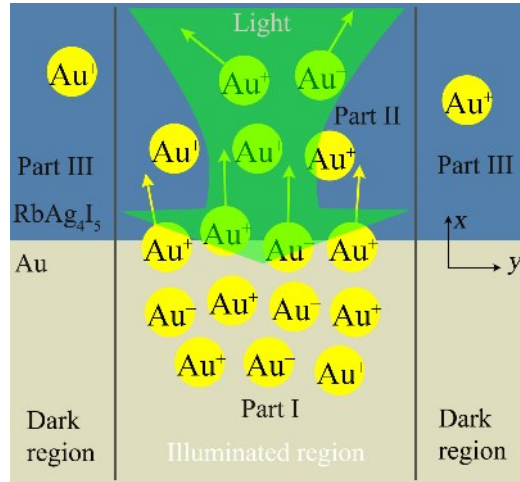


**Fig. S2.** The schematic diagram of Au<sup>+</sup> ionic diffusion from Au film to RbAg<sub>4</sub>I<sub>5</sub> film under illumination.

According to the equation of Fick's second law

$$\frac{\partial C}{\partial t} = \frac{\partial}{\partial x} \left( D \frac{\partial C}{\partial x} \right) \quad (1)$$

we use Matano method to calculate the relation between diffusion rate and concentration

$$D \propto \int_{C_0}^C x dC \quad (2)$$

We define the diffusion rate of Au<sup>+</sup> ions from Part I to Part II is  $D_1$  and the diffusion rate of Au<sup>+</sup> ions from illuminated region to non-illuminated region in RbAg<sub>4</sub>I<sub>5</sub> is  $D_2$ , both of which are proportional to the distance along the normal direction  $\hat{x}$ . According to Equation (2) and assumption 4, we can get  $dD_1/dx$  which is proportional to  $C_1-C_2$  and also time independent. Considering the Au<sup>+</sup> ionic diffusion from illuminated region to non-illuminated region in RbAg<sub>4</sub>I<sub>5</sub>, the resulted  $C_2$  is related to  $D_1$  and  $D_2$ . When Au<sup>+</sup> ions diffuse from Au film to RbAg<sub>4</sub>I<sub>5</sub>,  $C_2$  increases;

when  $\text{Au}^+$  ions diffuse from illuminated region to non-illuminated region in  $\text{RbAg}_4\text{I}_5$ ,  $C_2$  decreases. Hence, we can get the simplified Equation (1) about the change of  $\text{Au}^+$  ionic concentration  $C_2$  in  $\text{RbAg}_4\text{I}_5$ .

$$a(C_1 - C_2) - b(C_2 - C_3) = \frac{dC_2}{dt} \quad (3)$$

Where  $a$  is a constant proportional to  $dD_1/dx$  and  $b$  is a constant proportional to  $dD_2/dx$ . The first item on the left means the increased  $\text{Au}^+$  ions and the second item means the decreased  $\text{Au}^+$  ions. According to assumption 2 and 3,  $C_1$  is approximately stable and  $C_3$  is 0. Therefore, the solution of Equation (3) is

$$C_2 = C_1 \frac{a}{a+b} (1 - e^{-(a+b)t}) \quad (4)$$

On the other hand, when  $\text{Au}^+$  ions diffuse from Au film to  $\text{RbAg}_4\text{I}_5$ , the lost lattices in Au film will reduce the electrical transport channels. The declined current is  $\Delta I = U \Delta N / R_0 N$ , where  $\Delta N \propto \Delta C_1$  is the lost lattices,  $N$  is the initial number of Au lattices of composited Au film,  $U$  is the bias voltage and the total resistance is  $R_0$ . The differential form of  $N$  is

$$a(C_1 - C_2) \propto \frac{dN}{dt} \quad (5)$$

Then at time  $t$ , the change of  $C_1$  is

$$\Delta N(t) \propto C_{1,t=0} \frac{abt}{a+b} + C_{1,t=0} \frac{a^2}{(a+b)^2} (1 - e^{-(a+b)t}) \quad (6)$$

Where  $C_{1,t=0}$  is the initial  $\text{Au}^+$  ionic concentration in Au film. Considering the assumption 1 and the Equation (4), the finally decreased current as a function with time can be written as:

$$\Delta I = A(1 - e^{-t/\tau}) + Bt \quad (7)$$

Where  $A$  and  $B$  are both proportional constants, and  $\tau$  is the time constant which is equal to  $1/(a+b)$ . The first item on the right contains the influence of ionic scattering and lost lattices, and the second item is from the lost lattices which makes the dominated contribution to  $\Delta I$  when  $C_2$  approach saturation point.

### Section two. The model of SPP effects

The declined photocurrent of an Au film is related to the SPP effects which contains two aspects, SPP-induced heating and SPP-electron interaction. The characteristic time scale of SPP-electron interaction is far shorter than that of SPP-induced heating. So when we study the photocurrent as a function with continuous time for an Au film, it's convenient to rule out the first two data points which mainly contain the influence of SPP-electron interaction. The remained data points are easy to analyse according to the influence of SPP-induced heating. The heat will be produced continuously in the rough surface under illumination. And the Au film will be heated simultaneously, while the heat can also dissipate into surrounding environment. This thermal transmission process is similar to the ionic diffusion model. So the increased temperature of Au film  $\Delta T$  is proportional to  $(1 - e^{-t/\tau_0})$ , where the characteristic time  $\tau_0$  is related the processes of heat produce and heat

dissipation. The declined photocurrent can be expressed as

$$\Delta I = \alpha(1 - e^{-t/\tau_0}) + \beta \quad (8)$$

the first item on the right is from the increased temperature, and the second item is from the initial influence of SPP-electron interaction. According to our above analysis, we can model the declined photocurrent of an individual Au film, as Fig. S3 shows. The fitting matches well with our experimental results.

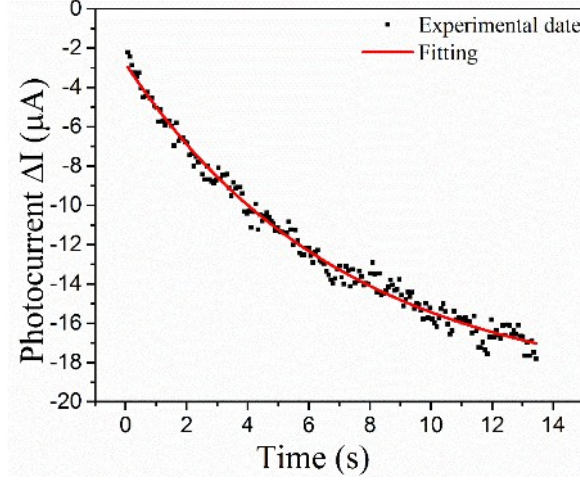


**Fig. S3.** The thickness of Au film is about 50 nm. The power density of the 532 nm laser is 4.8 mW/mm<sup>2</sup>. And the bias voltage is 0.2V.

### Section three. The final model of photoresponse

Fig. S4.a shows a complete photoresponse process of RbAg<sub>4</sub>I<sub>5</sub>/Au under illumination of 532 nm laser for a long time. Due to the continuously lost lattices, the declined photocurrent is several time larger than the recovered current. The recovered current is mainly resulted from the decreased Au<sup>+</sup> ionic concentration  $C_2$  in RbAg<sub>4</sub>I<sub>5</sub> and the recovery of losing lattices in Au film. In addition, the dissipation of SPP-induced heat also contributes the recovery of the current under dark condition. The change of  $C_2$  can be expressed as

$$a^* C_2 + b C_2 = \frac{dC_2}{dt} \quad (9)$$

$$C_2(t) = C_{2,t=0} e^{-(a^* + b)t}$$

Where  $a^*$  is related to the Au<sup>+</sup> ionic diffusion from RbAg<sub>4</sub>I<sub>5</sub> to Au film within the build-in electric field,  $C_{2,t=0}$  is the saturation concentration of Au<sup>+</sup> ions in RbAg<sub>4</sub>I<sub>5</sub> when the light is turned off, and  $b$  is same as Equation 3. Then the differential form of  $N$  can be expressed as

$$a^* C_2 \propto \frac{dN}{dt} \quad (10)$$

And we can get the total change of  $N$  through integral

$$\Delta N(t) \propto \frac{a^* C_{2,t=0}}{a^* + b} (1 - e^{-(a^* + b)t}) \quad (11)$$

$\Delta N$  is proportional to the increased current from the recovery of losing lattices. Considering the SPP effects, the total recovered current can be expressed as

$$\Delta I = A^*(1 - e^{-t/\tau_0}) + B^*(1 - e^{-t/\tau_1}) + \beta^* \quad (12)$$

Where  $\tau_1$  equal to  $1/(a^*+b)$  means the time decay constant of  $C_2$ ,  $A$  and  $B$  are both proportional constants and  $\beta^*$  is from the SPP-electron interaction. In order to simplify the process of fitting, we define  $\beta^*$  is equal to  $\beta$  in Equation (8) (In fact,  $\beta^*$  is larger than  $\beta$ . However,  $\beta^*$  is not much important in our model as a constant). Fig. S4.b shows the fitting result which matches well with the experimental dates. In addition, according to the final expression of  $\Delta I$  in Equation (12),  $B^*$  ( $\sim 43 \mu\text{A}$ ) is three time larger than  $A^*$  ( $\sim 14 \mu\text{A}$ ), that means the decrease of  $C_2$  make the dominated contribution to recovered current. Fig. S4.c shows the fitting result of initial diffusion model without consideration (Equation (7)) of SPP effects. The obvious mismatch means that the SPP effects are not negligible. If we take the SPP effects into consideration, the Equation (7) can be rewritten as

$$\Delta I = A(1 - e^{-t/\tau_2}) + A^*(1 - e^{-t/\tau_0^*}) + Bt + \beta \quad (13)$$

Under illumination, the characteristic time  $\tau_0^*$  is slightly different from  $\tau_0$ . Fig. S4.d shows the fitting result with SPP effects which is better than that in Fig. S4.c. And the time constant  $\tau_2$  (0.97 s), which indicates that the  $\text{Au}^+$  ionic diffusion from Au film to  $\text{RbAg}_4\text{I}_5$  is much faster than from  $\text{RbAg}_4\text{I}_5$  to Au film.

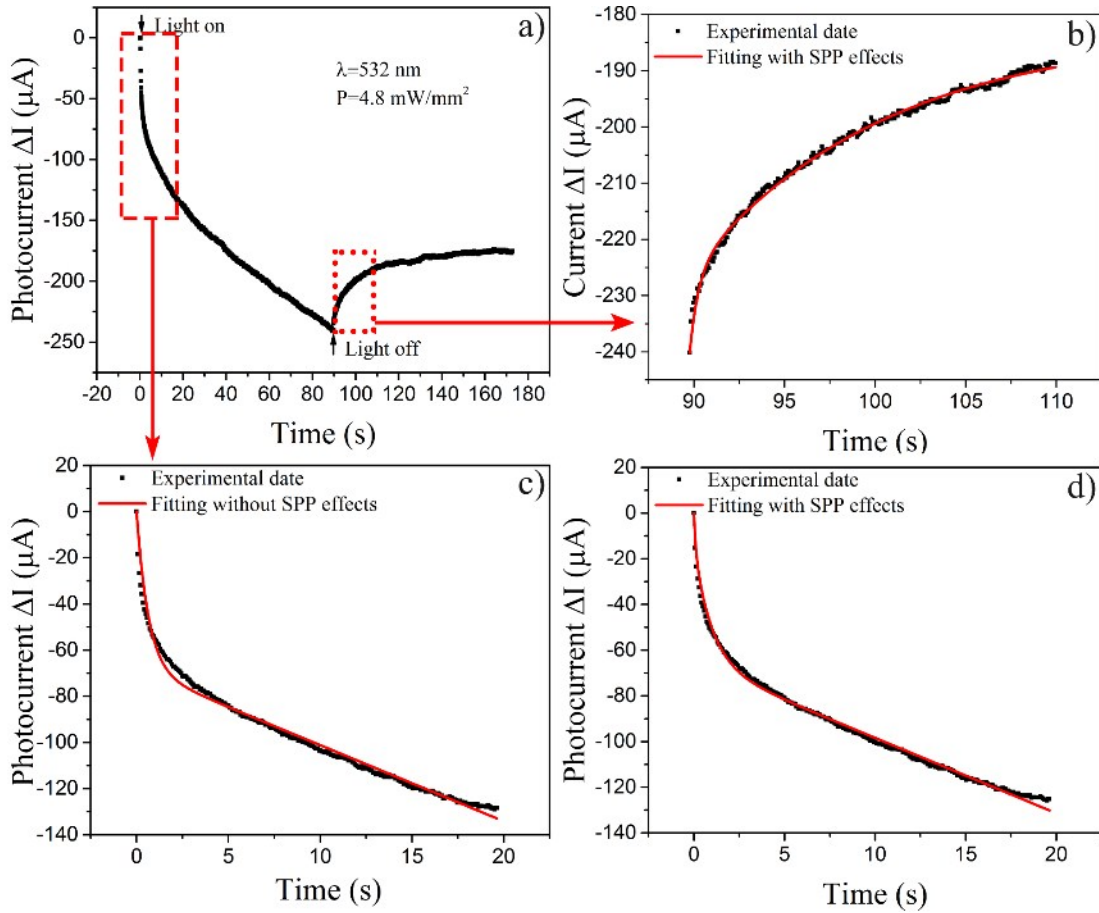


**Fig. S4.** (a) The photoresponse of  $\text{RbAg}_4\text{I}_5/\text{Au}$  for a long time. (b) The fitting of recovered current. (c) The fitting of declined photocurrent without consideration of SPP effects. (d) The fitting of declined photocurrent with consideration of SPP effects. The bias voltage is 0.2 V.

#### Section four. The photocurrent as a function with light power

According to the Equation (4), the  $\text{Au}^+$  ionic concentration  $C_2$  keeps unchanged if the time is same. If the illumination time is only 200 ms which is much smaller than the characteristic time  $\tau_2$  ( $\sim 1$  s), the lost lattices is negligible and the SPP-electron interaction is weak. Hence, under this condition, when we model the photocurrent of  $\text{RbAg}_4\text{I}_5/\text{Au}$  as a function with light power  $P$ , we can ignore the influences of the lost lattices and SPP effects. Under illumination of a same laser, the number of excited  $\text{Ag}^+$  ionic vacancies is proportional to light power  $P$ , which means the volume of region containing  $\text{Au}^+$  ions denoted as  $V$  is proportional to  $P$ . When the volume  $V$  is very small, it's reasonable to assume that each ion is equivalent. However, if the volume  $V$  is large, the scattering effect of  $\text{Au}^+$  ions far away from the interface become weak. Hence, it's necessary to correct the scattering effect of  $\text{Au}^+$  ions with a decay factor  $1/(l_0+l)^2$ , where  $l$  is the distance between  $\text{Au}^+$  ions in Part II and interface along the normal direction and  $l_0$  is nearest distance. The final expression of  $\Delta I$  is

$$\Delta I = \int_0^{l_1} R \frac{C_2 \cdot S dl}{(l_0 + l)^2} = RSC_2 \left( \frac{1}{l_0} - \frac{1}{l_0 + l_1} \right)$$

$$\Delta I = I_s \left( 1 - \frac{1}{1 + \gamma P} \right)$$
(14)

Where  $l_1$  is the farthest distance which is proportional to light power  $P$  and also related to wavelength,  $S$  is the section area composite nanostructure and  $R$  is the constant ratio of  $\Delta I$  to the total number of  $\text{Au}^+$  ions in Part II.  $I_s$  is the saturation value of  $\Delta I$ , and  $\gamma$  is a proportional constant related to  $l_0$  and wavelength. According to our analysis, when the number of  $\text{Au}^+$  ions in Part II approaches the saturated number, the influence of the following added ions is weak enough to be ignored since the operating distance is too far. Therefore, the saturation values of  $\Delta I$  should be equal under illumination of different lasers.

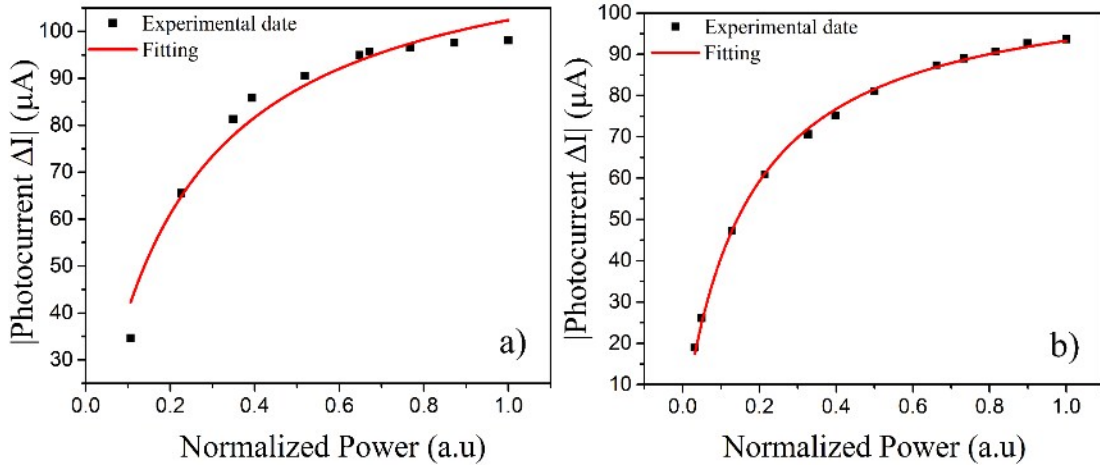


**Fig. S5.** (a) Fitting result for 405 nm. (b) Fitting result for 532 nm. The time of illumination is 200 ms and the bias voltage is 0.2 V.

Fig. S5.a shows the fitting result of photocurrent as a function with light power at wavelength of 405 nm and Fig. S5.b shows the fitting result at wavelength of 532 nm. The fitted saturation values of photocurrent for above two lasers are approximately equal ( $\sim 120 \mu\text{A}$  for 405 nm and  $\sim 110 \mu\text{A}$  for 532 nm) which means the saturated numbers of  $\text{Au}^+$  ions under different lasers' illumination are approximately same. The slight difference may be from  $C_2$ , because we treat the  $\text{Au}^+$  ionic



concentrations  $C_2$  as same with different lasers. However, as an important parameter for the expression of  $C_2$  in Equation (3),  $a$  is slightly different since the  $\text{Ag}^+$  ionic vacancy densities are different with different lasers.

1. J. Bardeen, *Physical Review*, 1947, **71**, 717-727.
2. D. Chattopadhyay and H. J. Queisser, *Reviews of Modern Physics*, 1981, **53**, 745-768.
3. C.T.Sah, T.H.Ning and L.L.Tschopp, *Surface Science*, 1972, **32**, 561-575.

## Verification of the Transportation of $\text{Au}^+$ Ions in $\text{RbAg}_4\text{I}_5$

An Au film and an Al film were deposited on the opposite sides of quartz glass substrate as an anode and a cathode respectively, through thermal evaporation. Then the sample was coated with  $\text{RbAg}_4\text{I}_5$  completely by thermal evaporation deposition. Next, an electric field with bias of 140 V had been applied between the anode and the cathode for 10 min. Fig. S6.a shows the experimental schematic diagram. Some gold nanobranches grew beside the aluminum cathode. Fig. S6.b shows the transportation of  $\text{Au}^+$  ions from gold anode to aluminum cathode. Fig. S6.c shows the scanning electron microscope (SEM) characterization results of gold nanobranches at cathode after applying electric field. Fig. S6.d shows local energy dispersive spectrometer (EDS) of the nanobranches, which displays abundant components of Au. Combining these results, we can draw a conclusion the ionized  $\text{Au}^+$  ions transport from anode to cathode and then are reduced at aluminum cathode. Totally, we confirmed the transportation of  $\text{Au}^+$  ions in  $\text{RbAg}_4\text{I}_5$ .

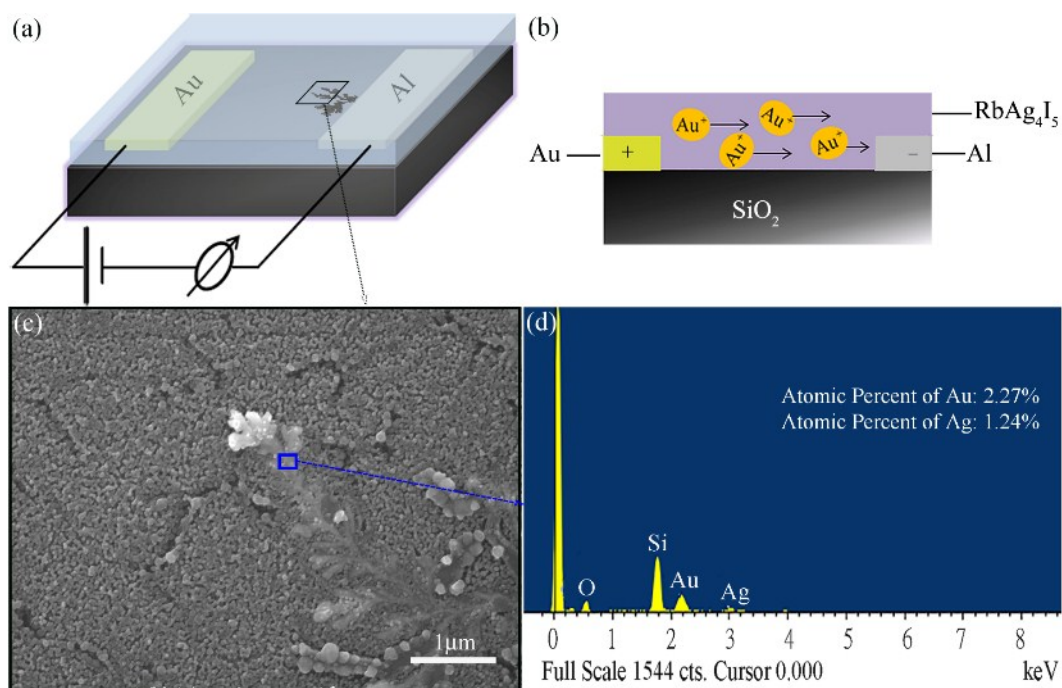


**Fig. S6.** (a) The experimental schematic diagram. Gold is an anode electrode and aluminum is a cathode electrode. The thickness of Au film and Al film is both about 30 nm and the gap width between them is 0.5 mm. The thickness of  $\text{RbAg}_4\text{I}_5$  is about 100 nm. (b) The transportation schematic diagram of ionized  $\text{Au}^+$  ions from gold anode to aluminum cathode. (c) SEM image of reduced gold nanobranches at cathode. (d) The local EDS of the reduced gold nanobranches.

### Photoresponse of RbAg<sub>4</sub>I<sub>5</sub>/Au with a thicker Au film

As Figure S7.a shows, the photoresponse curve is very similar with Figure 4a in our paper. Because the dominant contribution of the photocurrent is from Au<sup>+</sup> ions scattering effect. When the thickness of an Au film is increased beyond a critical value  $d_1$ , the fraction of Au film influenced by the Au<sup>+</sup> ionic is stable due to the limited operating distance of Coulomb interaction. So the final saturated photocurrent of a device containing a thicker Au film (45 nm) is almost equal to that of a device containing a thinner Au film (30 nm).

However, when the thickness of an Au film is increased, the dark current is also increased. In our experiments, the dark current for a device with a 30-nanometer-thick Au film is 4.1 mA, while the dark current for a device with a 45-nanometer-thick Au film is 12.2 mA. For the condition of a thicker Au film, the ratio of photocurrent to dark current ( $|\Delta I|/I_{dark}$ ) may be decreased which is harmful to the performance of a device. In addition, when we reduce the thickness of Au film to an enough small value  $d_2$ , the current may be cut off owing to the discontinuous Au particles.

When the thickness of an Au film is in between  $d_1$  and  $d_2$ , the whole Au film in the illuminated region can be effected by the Au<sup>+</sup> ions owing to the significant Coulomb interaction. Hence, the photocurrent of a device under short-wavelength illumination will be larger with the increase of an Au film's thickness.

As Figure S7.b shows, the absolute value of photocurrent  $|\Delta I|$  of this thicker device is larger than that of the thinner device, but the whole photoresponse curve is similar. Since the Au film is constituted of Au particles, from ultraviolet to near-infrared, the transmittance of the Au film is larger than 0.5 even at a thickness of 45 nm. Hence, the operating depth of the light is same as the thickness of the Au film. As a result, with a same light illumination, an Au film with thickness of 45 nm can be excited stronger SPPs than an Au film with thickness of 30 nm. Finally,  $|\Delta I|$  of this thicker device is increased.

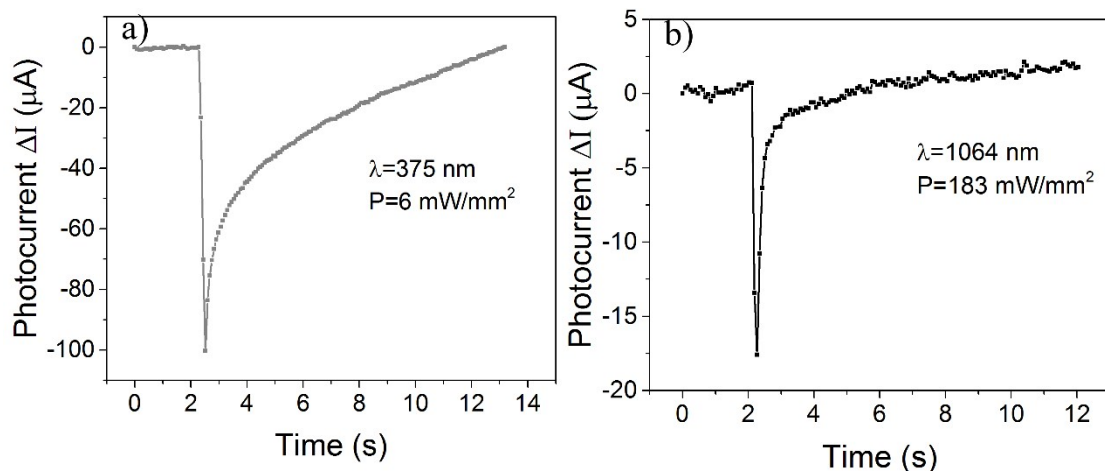


**Figure S7.** The photoresponse curve of RbAg<sub>4</sub>I<sub>5</sub>/Au under illumination of lasers with wavelength at (a) 375 nm, (b) 1064 nm. The thickness of Au film is about 45 nm.